

Soft X-ray Beamline Specialized for Actinides and Radioactive Materials Equipped with a Variably Polarizing Undulator

A. Yokoya,* T. Sekiguchi, Y. Saitoh, T. Okane, T. Nakatani, T. Shimada, H. Kobayashi,† M. Takao, Y. Teraoka, Y. Hayashi, S. Sasaki,‡ Y. Miyahara, T. Harami and T. A. Sasaki

Japan Atomic Energy Research Institute, Akou-gun, Hyougo-ken 678-12, Japan.

E-mail: yokoya@sp8sun.spring8.or.jp

(Received 4 March 1997; accepted 16 July 1997)

This report presents the design of an undulator beamline at SPring-8 to be used for soft X-ray spectroscopy focused on radioactive materials. Photoemission spectroscopy experiments are carried out in a radioisotope (RI)-controlled area where actinide compounds as well as unsealed radioactive materials are usable. Intrusion of the radioactive materials into the electron storage ring or to the outside of the evacuated beamline components can be avoided by a specially devised RI protection/inspection mechanism. The combination of a variably polarizing undulator and a varied-line-spacing plane-grating monochromator provides linearly or circularly polarized soft X-rays with a high resolving power in the energy range 0.28–1.5 keV. The beamline will become operational in December 1997.

Keywords: radioactive materials; actinides; soft X-ray spectroscopy; circular polarization; variably polarizing undulators.

1. Introduction

Synchrotron radiation with monochromatized energy in the soft X-ray range is a powerful light source for electron spectroscopy, photochemical reactions and so on. In the past decades soft X-ray photoelectron spectroscopy has been applied to the study of highly correlated electron systems that show a great variety of physical properties such as electrical conductivity, magnetism *etc.* The actinides are among materials belonging to highly correlated electron systems, but understanding of their electronic structures is especially poor (Baer, 1984; Arko *et al.*, 1987; Allen, 1992). One of the reasons for this is the difficulty in handling unsealed radioactive isotopes (RI), including actinides, at synchrotron radiation facilities, because we need some counter-measures against RI pollution of experimental devices as well as facility users. Although beamlines for studying RI materials are preferably constructed in areas specialized for experiments with RI samples, such beamlines are not common at current synchrotron radiation facilities. Recently, we have installed a bending-magnet beamline for radioactive materials at the Photon Factory in the National Laboratory for High Energy Physics (Konishi *et al.*, 1996). This beamline provides photons whose energies range from 1.8 to 6.0 keV. In the VUV energy region an undulator beamline covering 80–1200 eV is under operation at the Advanced Light Source, Lawrence Berkeley

Laboratory (Padmore & Warwick, 1994). The beamline achieved a small-size beam with high flux which is available for photoemission spectroscopy of trace amounts of curium. Photon beams obtained from these beamlines on axis are just linearly polarized.

We have designed a soft X-ray undulator beamline for electron spectroscopy studies of actinide materials, as well as for other applications of site-selective photochemical processes of surface molecules or in biological systems. The beamline will be located at the high-brilliance synchrotron radiation source, SPring-8, based on the following points.

(i) The experimental station for actinide samples will be placed in a building that is separated from the common experimental hall and will be referred to as the 'hot sample area'.

(ii) The beamline will be equipped with special apparatus to protect the users, the experimental devices and the storage ring from intrusion of radioisotope pollution.

(iii) Monitoring systems for radioactivity inside the evacuated devices will be placed at several points on the beamline.

(iv) To obtain a high resolving power of circularly and linearly polarized soft X-rays at the sample position, the combination of a grating monochromator and a variably polarizing undulator has been chosen.

2. Layout of the beamline

The beamline components are to be installed in the BL23SU section of SPring-8, as shown in Fig. 1. The beamline has

† Present address: Shin-Etsu Chemical Company Ltd, Kitago, Takefu, Fukui 915, Japan.

‡ Present address: ALS, LBNL, Berkeley, CA 94720, USA.

Table 1
Apparatus for RI protection/inspection.

Device	Distance from light source (m)	Function
FGV1	33.2	Vacuum protection against shock waves
Cold cathode gauge 1	33.5	Sensor of FGV1
RI port 1	33.8	RI inspection
FGV2	73.9	Vacuum protection against shock waves
RI port 2	89.5	RI inspection
ADL	92–108	Acoustic delay function
RI port 3	110.4	RI inspection
FGV3	111.0	Vacuum protection against shock waves
Cold cathode gauge 2	113.2	Sensor of FGV2 and FGV3
Cold cathode gauge 3	114.6	Sensor of FGV2 and FGV3

three experimental stations in a tandem fashion: the actinide science station, the surface photochemistry station and the biological applications station. A distinctive feature of the beamline is that the actinide science station is located in a building, the hot sample area (HSA), which is separated from the normal experimental hall. The other two stations are in the normal experimental hall.

Prefocusing mirrors and a monochromator to obtain a high resolving power of soft X-rays are set at 40–70 m from the light source in the normal hall. Details of the optics are described in §6.

3. Special apparatus to protect the beamline from RI pollution

The beamline has various mechanisms to protect the users, the experimental devices and the storage ring from the intrusion of RI pollution. This special apparatus is listed in Table 1 with its functions and distances from the light source.

3.1. Acoustic delay line

Shock waves formed by a momentary air leakage in the vacuum chamber in the actinide science station bring the RI samples upstream of the beamline. In order to prevent the intrusion of the waves, an acoustic delay line (ADL) is installed in the space between the two buildings, namely the experimental hall and the HSA.

The ADL consists of a long beam-transport pipe containing 12 disks, as shown in Fig. 2. The total length of the pipe is about 16 m. The inner diameter of the pipe is 35 mm except for the disk section. The pressure in the ADL is kept to 1.3×10^{-3} Pa. At this pressure the velocity of the acoustic waves in the ADL is estimated to be 1500 m s^{-1} using a numerical analysis code of axisymmetric compressible flow, indicating that the acoustic waves take about 11 ms to travel through the ADL.

3.2. RI defense mechanisms

Three pneumatic fast-closing gate valves (FGV1, FGV2 and FGV3 in Table 1) are also immediately closed within

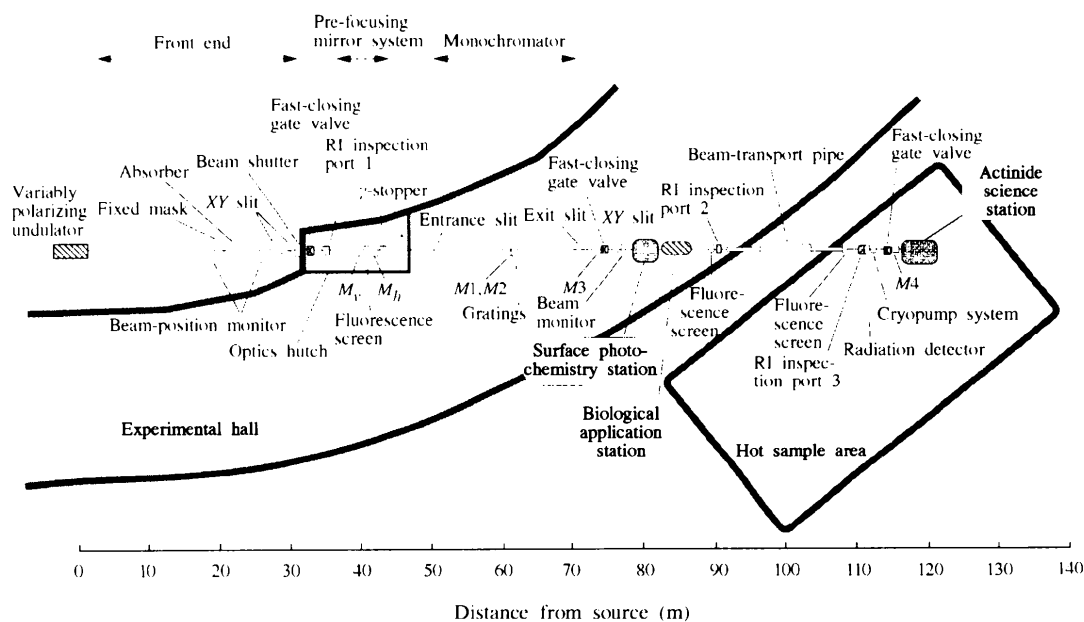


Figure 1
Schematic illustration of the layout of the whole beamline system on BL23SU.

10 ms when the FGV sensors detect a pressure rise in the vacuum chamber. The distances of the valves from the actinide science station in the HSA, which is thought to be a source of RI materials, are about 5.5, 41 and 82 m. Double cold cathode gauges used as sensors of both FGV2 and FGV3 are placed within 2 m of the actinide science station, as shown in Fig. 3. FGV2 and FGV3 are operated by trigger signals generated by the gauges. FGV1 and its sensor are placed in the optics hutch.

The beam-transport section, including several apparatus such as the fluorescence-screen monitor chamber in the HSA, is also expected to have an acoustic delay function. Acoustic waves entering from the experimental station will be blocked by FGV3. The waves which pass through FGV3 before the valve closes travel in the beam-transport section in the HSA and ADL. It takes over 10 ms before the waves

reach FGV2, as mentioned in §3.1. This means that the acoustic waves are completely blocked by the two FGVs. The final pressure rise will therefore not occur upstream of the beamline, the front end and the storage ring.

3.3. RI inspection apparatus

The RI inspection port enables the inspection of radioactivity inside the beamline without breaking the ultra-high vacuum of the chamber (Konishi *et al.*, 1996). A newly designed port for the beamline consists of two vacuum chambers with a simple mechanism to transport a mask for RI inspection. The port is schematically drawn in Fig. 4. The aperture size is 20×20 mm.

One port is placed in the HSA and two ports are placed in the experimental hall. The mask is taken out of the chamber for a smear test with a liquid scintillation counter. The detection efficiency of the counter is over 50% and the background level is $10 \text{ counts min}^{-1}$. For example, the minimum detection level of ^{237}U , which has the shortest lifetime of the uranium isotopes, is about 4×10^{-16} g on the mask surface.

4. Light source

A variably polarizing undulator, called 'APPLE II' (Sasaki, Miyata & Takada, 1992; Sasaki *et al.*, 1993; Sasaki, 1994; Kobayashi *et al.*, 1996), is installed in the storage ring to obtain both linearly and circularly polarized soft X-rays. The minimum gap of the magnets is 36 mm. The magnetic period length is 120 mm and the number of periods is 16. The spectral data calculated by the synchrotron radiation calculation program *URGENT* (Walker & Diviacco, 1992) are shown in Fig. 5.

The energy range of soft X-rays from 0.28 to 1.5 keV in the horizontal polarization mode and from 0.5 to 1.5 keV in the circular polarization mode is covered by the first harmonic. To make high-sensitivity measurements of circular dichroism, the right and left circular polarizations

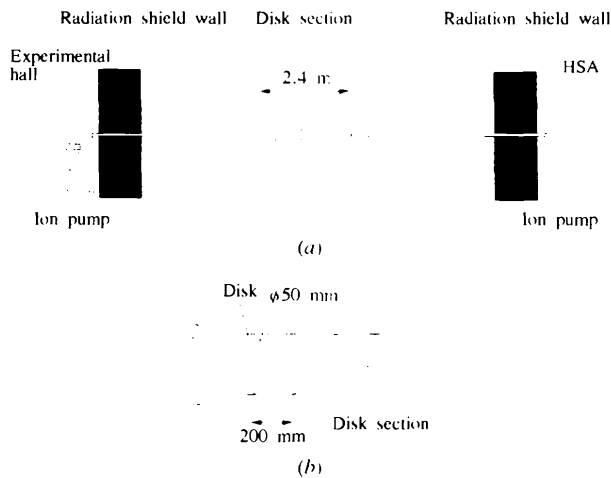


Figure 2
Schematic illustration of (a) the whole acoustic delay line connecting the normal experimental hall and the HSA, and (b) the disk structure in the ADL. 12 disks with apertures of diameter 50 mm are in the pipe.

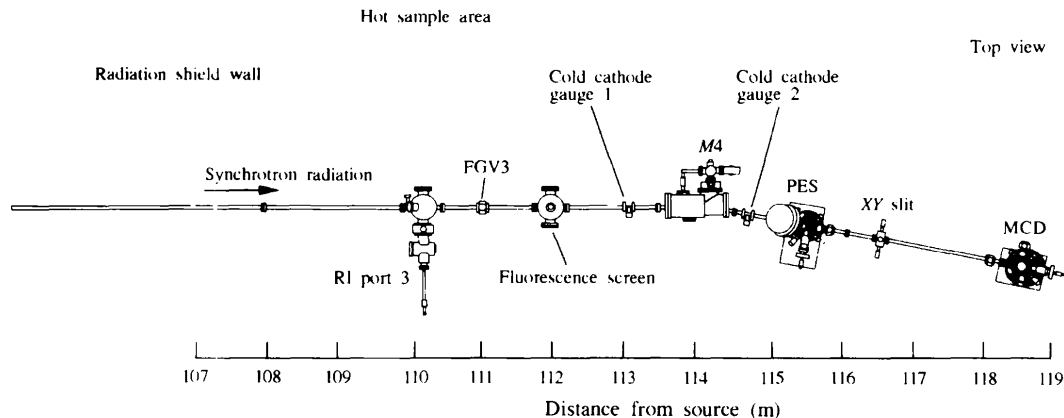


Figure 3
Layout of the devices in the HSA. The actinide science station consists of the MCD and PES at the end of the beamline. These UHV chambers are set at the focusing points of the $M4$ mirrors. The RI port and FGV are special devices for RI protection/inspection.

Table 2
Specifications of the variably polarizing undulator.

Type	Variably polarizing undulator		
Period length (mm)	120		
Number of periods	16 poles		
Total length (mm)	1920		
Circular polarization mode			
Magnet gap (mm)	39	54	58
K value	3.0	2.0	1.5
First harmonic energy (keV)	0.5	1.0	1.5
Total radiation power (kW)	1.1	0.49	0.27
Horizontal polarization mode			
Magnet gap (mm)	36	63	73
K value	5.8	2.8	2.2
First harmonic energy (keV)	0.28	1.0	1.5
Total radiation power (kW)	2.1	0.49	0.27
Brilliance [photons s^{-1} mrad $^{-2}$ mm $^{-2}$ (0.1% bandwidth) $^{-1}$ (100 mA) $^{-1}$]	$> 2 \times 10^{17}$		

are alternately changed at 0.5 Hz by adjusting the phase shift. The specifications of the undulator are listed in Table 2.

5. Beam monitors at the front end

To measure the beam profile and its centre, a pair of photon-profile monitors of carbon-wire-type (Zhang, Sugiyama, Ando, Xia & Shiwaku, 1995) are installed at 18 and 26 m from the light source. The change of the photon-beam position or direction caused by the magnetic field error of the undulator at each gap or phase will be calculated using the signals from the photon monitor and electron-beam-position monitors. The series of data will be stored to be

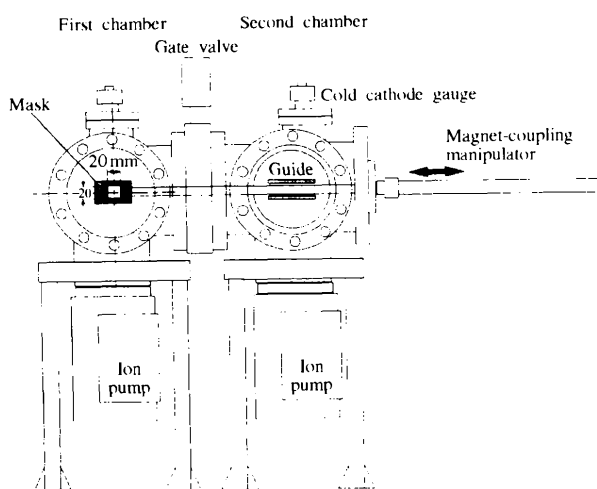


Figure 4
Schematic illustration of a radioisotope inspection port with two vacuum chambers separated by a gate valve. A mask with an aperture size of 20 (H) \times 20 (W) mm for the RI survey is transported by a magnet-coupling manipulator between the chambers.

used as parameters to control two steering magnets, which are set just upstream and downstream of the undulator, to cancel the magnetic field error.

A beam-position monitor consisting of a graphite filter is installed at the upper stream of the fixed mask in an interlocking system to avoid beam irradiation on the inside wall of the beam-transport duct. As shown in Fig. 6, the position monitor has an elliptical aperture to be able to detect a beam direction fluctuation of ± 200 μ rad in both linear and circular polarization mode.

6. Optics

We adopted the basic concept of the monochromator for the SPring-8 public beamline BL25SU for an electron spectroscopy study of condensed matter (Taniguchi, Suga, Daimon

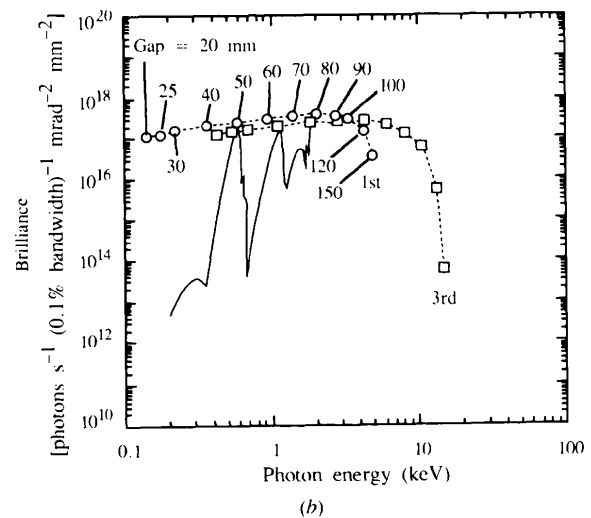
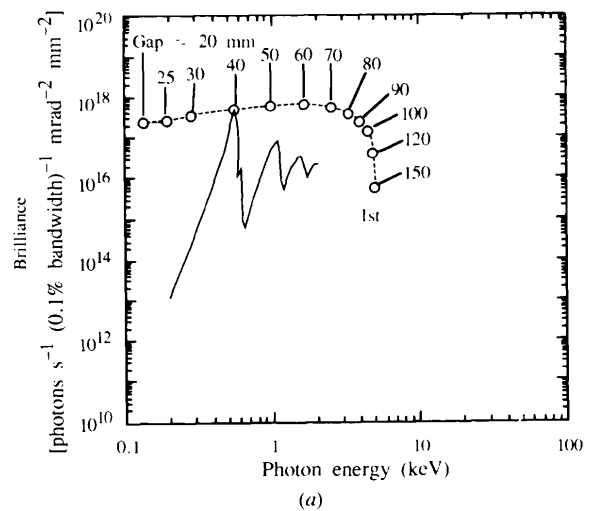


Figure 5
Brilliance of the undulator radiation as a function of gap width in (a) circular polarization mode ($\lambda_u = 120$ mm, $N = 16$), and (b) linear polarization mode ($\lambda_u = 120$ mm, $N = 16$). The solid lines indicate the spectrum when the magnet gap is (a) 40 and (b) 50 mm.

& Fujisawa, 1994; Iwami, Taniguchi, Suga & Saitoh, 1995; Saitoh, 1996). The monochromator is equipped with three varied-line-spacing plane gratings (Fujisawa *et al.*, 1996), which cover the energy region from 0.28 to 1.5 keV. A schematic illustration of the monochromator and the focusing mirror is shown in Fig. 7. The energy resolution of the monochromator, $E/\Delta E$, will be greater than 10^4 over the whole energy range.

The cylindrical Si mirror, M_v , and the plane Si mirror, M_h , are placed at 40 and 42.5 m from the source, respectively. A sagittal-focusing system is adopted for M_v , which focuses the beam on the entrance slit in the vertical direction. M_h focuses in the horizontal direction with a mechanical bending system. The incident angle of the beam on the mirrors is 88.5° . The power density on M_v is about 0.86 W mm^{-2} when the K value of the undulator is 5.8.

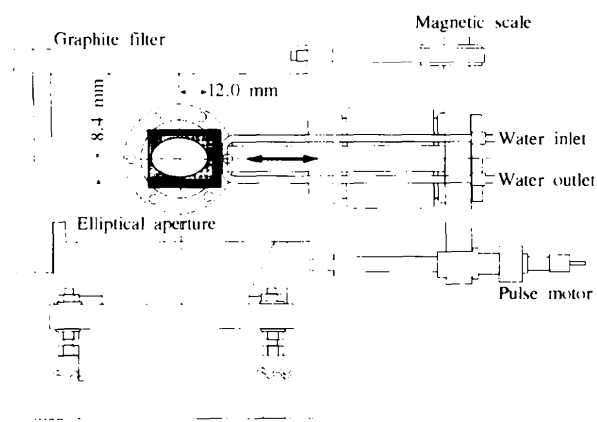


Figure 6

Beam-position monitor for an interlocking system. The thickness of the graphite filter is about $100 \mu\text{m}$. The elliptical aperture can be moved by a motor-drive system to remove it from the beam axis.

The water-cooled mirror-holder system that is adopted for M_v and M_h will efficiently reduce the heat load on the mirrors. The cylindrical mirror, M_3 , and toroidal mirror, M_4 , are used to refocus the beam on the actinide science station. Specifications of the optical components are listed in Table 3. The horizontal and vertical FWHM beam sizes are less than 1.0 and 0.5 mm, respectively, at the actinide science station and 2.0 and 1.0 mm, respectively, at the surface photochemistry and biological application stations. The photon flux is expected to be greater than 10^{11} photons s^{-1} at the stations.

7. Experimental stations

In the actinide science station at the HSA we will make magnetic circular dichroism (MCD) measurements of ferromagnetic actinide compounds and photoelectron spectroscopy (PES) experiments of heavy-fermion compounds with high energy resolution to clarify the physical properties of actinide compounds from the viewpoint of electronic structures. The arrangement of these devices in the HSA is shown in Fig. 3.

One of the advantages of the experimental station is the utilization of variable polarization produced with a state-of-the-art insertion device. Application of the plural experimental techniques using different kinds of polarization is very helpful for the systematic study of electron spectroscopy. For example, we can make both measurements of the MCD using circular polarization and angle-resolved photoemission using linear polarization for a single-crystal ferromagnetic sample. These kinds of experiments promote understanding of the electronic structure with information from various aspects.

Applications of highly brilliant soft X-rays also provide some advantages for surface photochemical and radiobiological research in the normal experimental hall. In order

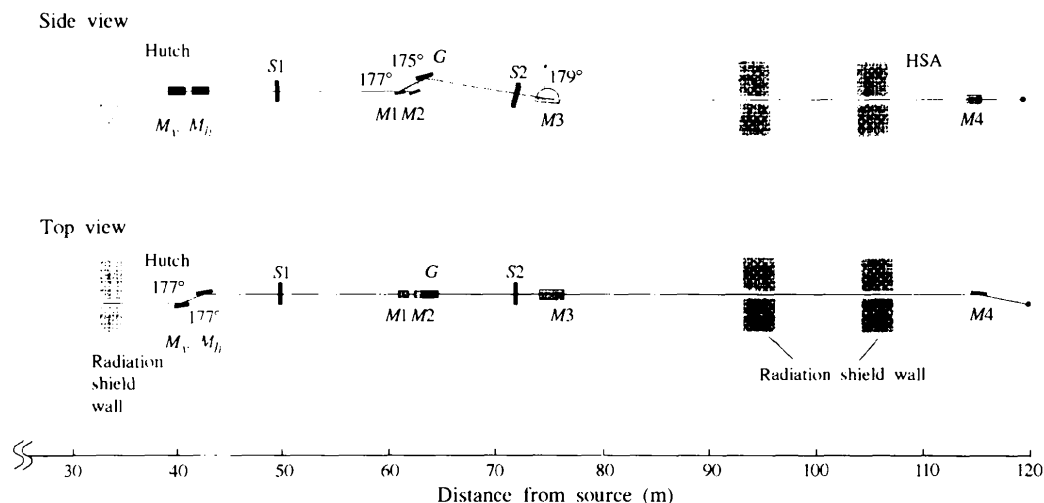


Figure 7

Layout of the optical components of the high-resolution-type monochromator equipped with three varied-line-spacing plane gratings. Two spherical mirrors, M_1 and M_2 , are switched to obtain the proper photon energy.

Table 3
Specifications of the optical components.

Distance from source (m)	Optical element	Size (L × W × T) (mm)	Angle of incidence (°)
40	Cylindrical mirror (M_1) with a water cooling system	450 × 40 × 40	88.5
42.5	Plane mirror (M_h) with a water cooling system and a bent system	500 × 40 × 30	88.5
60.955	Spherical mirror ($M1$) with a water cooling system	350 × 40 × 40	88.5
61.338	Spherical mirror ($M2$) with a water cooling system	350 × 40 × 40	87.5
61.9	Varied-space plane gratings with a water cooling system	220 × 50 × 20	$\alpha + \beta = 176$ ($M1$) $\alpha + \beta = 174$ ($M2$)
73.91	Cylindrical mirror ($M3$)	500 × 40 × 50	89.5
114	Toroidal mirrors ($M4$)	250 × 40 × 30	88.5

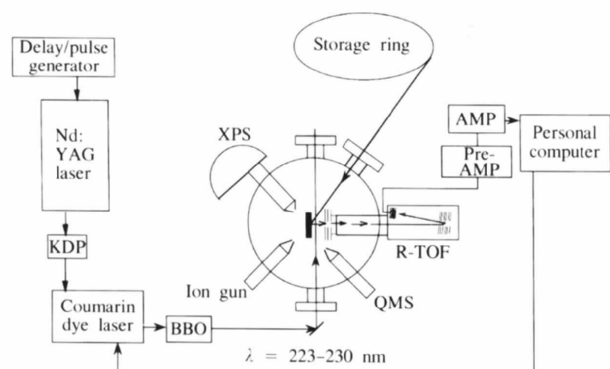


Figure 8

Schematic diagram of the resonantly enhanced multiphoton ionization (REMPI) detection system to be installed in the surface photochemistry station. KDP and BBO represent potassium dihydrogenphosphate and β -barium borate crystals, respectively. QMS is a quadrupole mass spectrometer, R-TOF is a reflection-type time-of-flight mass spectrometer and AMP is an adjustable gain amplifier.

to obtain further information about photon-stimulated desorption, two detection systems, a resonantly enhanced multiphoton ionization (REMPI) system and an electron-ion coincidence system, will be developed for analysis of the desorption mechanisms of neutral and ionic species, respectively. Fig. 8 shows the surface photochemistry station schematically.

A schematic illustration of the biological application station is shown in Fig. 9. Inner-shell photoabsorption cross sections of carbon, nitrogen and oxygen in the biological samples will be measured by using a photodiode detection system. A paramagnetic resonance (EPR) apparatus is also installed for *in situ* detection of rare radical species as intermediate products in DNA-related molecules or amino acids at low temperatures.

We are grateful to Professor S. Suga of Osaka University and Dr Fujisawa of the University of Tokyo for their helpful assistance in designing the monochromator.

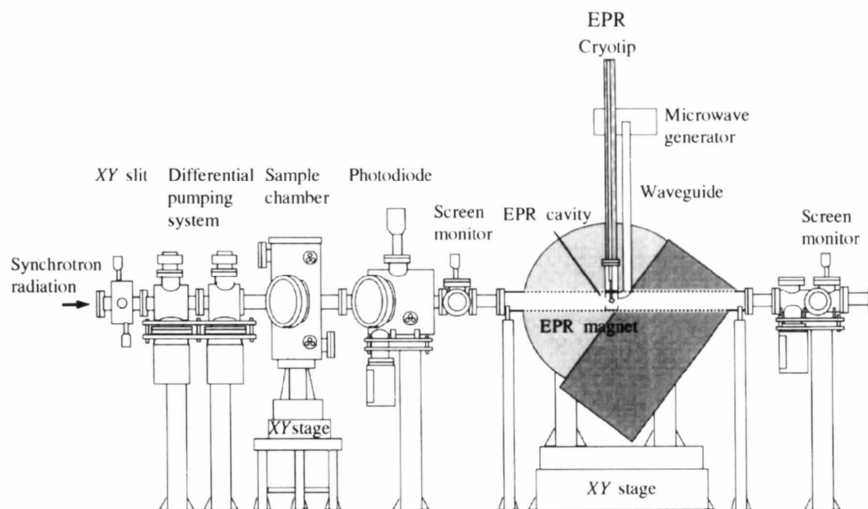


Figure 9

Schematic illustration of the station for biological applications. The EPR cavity and the irradiation apparatus are connected by a beam-transport pipe. These are evacuated by a differential pumping system.

References

- Allen, J. W. (1992). *Synchrotron Radiation Research: Advances in Surface and Interface Science*, Vol. 1, *Techniques*, ch. 6, edited by R. Z. Bachrach. New York: Plenum.
- Arko, A. J., Yates, B. W., DunLap, B. D., Koelling, D. D., Mitchell, A. W., Lam, D. J., Zolnierok, Z., Olson, C. G., Fisk, Z., Smith, J. L. & del Giudice, M. (1987). *J. Less-Common Met.* **133**, 87-97.
- Baer, Y. (1984). *Handbook on the Physics and Chemistry of Actinides*, ch. 4, edited by A. J. Freeman & G. H. Lander. Amsterdam: Elsevier Science.
- Fujisawa, M., Harasawa, A., Agui, A., Watanabe, M., Kakizaki, A., Shin, S., Ishii, T., Kita, T., Harada, T., Saitoh, Y. & Suga, S. (1996). *Rev. Sci. Instrum.* **67**, 345-349.
- Iwami, M., Taniguchi, M., Suga, S. & Saitoh, Y. (1995). *SPring-8 Annual Report*, pp. 57-60. SPring-8, Kamigori-cho, Ako-gun, Hyogo 678-12, Japan.
- Kobayashi, H., Sasaki, S., Shimada, T., Takao, M., Yokoya, A. & Miyahara, Y. (1996). *Proc. Eur. Accel. Conf.* **3**, 2579-2581.
- Konishi, H., Yokoya, A., Shiwaku, H., Motohashi, H., Makita, T., Kashiwara, Y., Hashimoto, S., Harami, T., Sasaki, T. A., Maeta, H., Ohno, H., Maezawa, H., Asaoka, S., Kanaya, N., Ito, K., Usami, N. & Kobayashi, K. (1996). *Nucl. Instrum. Methods*, **A372**, 322-332.
- Padmore, H. A. & Warwick, T. (1994). *J. Synchrotron Rad.* **1**, 27-36.
- Saitoh, Y. (1996). *SPring-8 Project Science Program*, Vol. 3, pp. 67-68. SPring-8, Kamigori-cho, Ako-gun, Hyogo 678-12, Japan.
- Sasaki, S. (1994). *Nucl. Instrum. Methods*, **A347**, 83-86.
- Sasaki, S., Kakuno, K., Takada, T., Shimada, T., Yanagida, K. & Miyahara, Y. (1993). *Nucl. Instrum. Methods*, **A331**, 763-767.
- Sasaki, S., Miyata, K. & Takada, T. (1992). *Jpn. J. Appl. Phys.* **31**, L1794-1796.
- Taniguchi, M., Suga, S., Daimon, H. & Fujisawa, M. (1994). *SPring-8 Annual Report*, p. 191. SPring-8, Kamigori-cho, Ako-gun, Hyogo 678-12, Japan.
- Walker, R. P. & Diviacco, B. (1992). *Rev. Sci. Instrum.* **63**, 392.
- Zhang, X., Sugiyama, H., Ando, M., Xia, S. & Shiwaku, H. (1995). *Rev. Sci. Instrum.* **66**, 1990-1992.